Progress In Electromagnetics Research, Vol. 123, 189–204, 2012

EXPERIMENTAL COMPARISON OF REMEDIAL SINGLE-CHANNEL OPERATIONS FOR REDUNDANT FLUX-SWITCHING PERMANENT-MAGNET MOTOR DRIVE

W. Zhao[1,*], M. Cheng[2], R. Cao[2], and J. Ji[1]

[1]School of Electrical and Information Engineering, Jiangsu University, No. 301, Xuefu Road, Zhenjiang, China

[2]School of Electrical Engineering, Southeast University, No. 2, Si-pai-lou, Nanjing, China

Abstract—Redundant flux-switching permanent-magnet (R-FSPM) motor is a new fault-tolerant machine having PMs in the stator, offering high efficiency, high reliability, and robust structure. This paper proposes two remedial control strategies for fault-tolerant operations of the R-FSPM motor drive in the single-channel (SC) mode. First, by doubling the healthy-channel currents, the reduced torque due to one channel loss can be remedied, the so-called remedial brushless AC (BLAC) operation mode. Second, by injecting harmonic current (IHC) considering harmonic back-EMF effect, the reduced torque can also be smoothly remedied, the so-c alled remedial IHC operation mode. Finally, both of the proposed remedial control strategies are verified by co-simulation and experimentation, hence confirming the validity of the proposed fault-tolerant R-FSPM motor drive.

1. INTRODUCTION

With the requirements for reducing emissions and improving fuel economy, electric vehicles (EVs) have attracted more and more attentions. High reliability is an essential requirement for electric propulsion of EVs, where any types of fault would lead to disastrous effects on life safety [1]. Hence, fault-tolerant operation of motor drives has been a growing demand [2].

Received 4 November 2011, Accepted 16 December 2011, Scheduled 20 December 2011

* Corresponding author: Wenxiang Zhao (zwx@ujs.edu.cn).

Permanent-magnet (PM) brushless motor drives are attracting extensive attention in high reliability applications, which are good candidates for EV applications [3–5]. By employing an arrangement of alternately wound teeth in the stator, a fractional-slot concentrated-windings PM machine, termed as rotor-PM machine, was proposed for fault-tolerant operation [6]. To operate the rotor-PM motor at flux weakening mode, an optimal torque control strategy was proposed in [7]. In addition, multi-phase PM motors have received great attention for fault-tolerant operation. In [8, 9], a new five phase motor drive was proposed. The proposed control guarantees safe drive operation considering the 3rd harmonic components of back-electromotive-force (back-EMF). However, since PMs are located in the rotor, these conventional rotor-PM brushless machines, including the surface-mounted, inset and interior topologies, suffer from weak mechanical structure and difficulty of PM cooling [10].

Recently, a new class of doubly-salient motors having PMs in the stator, termed as stator-PM motors, has been proposed and investigated [11]. These stator-PM motors include the doubly-salient PM (DSPM) type, flux-reversal PM (FRPM) type and flux-switching PM (FSPM) type. Extensive research work has been performed to analyze this class of machines, showing that stator-PM motors incorporate the merits of high power density, strong mechanical integrity and good immunity from thermal problem. It has been identified that the DSPM motors can inherently offer fault-tolerance [12]. Meanwhile, it has been verified that the FSPM motor can offer significantly higher power density than other stator-PM motors [13–15]. Very recently, by introducing the redundant technique to the FSPM machine topology, a new redundant FSPM (R-FSPM) motor has been proposed [16]. It is most viable for fault-tolerant operation of EVs, since it inherently offers high efficiency, high power density, maintenance-free operation, insignificant thermal influence on PMs and mechanically robust. Also in [16], control strategies for post-fault operation of up to two coils (not in the same channel, e.g., coils-A1 and -B2) have been investigated. However, it can't handle the fault of two or three coils in the same channel, such as coils-A1 and -B1.

The purpose of this article is to propose two remedial control strategies for fault-tolerant operations of the R-FSPM motor drive in the single-channel (SC) operation mode. The structure and electromagnetic features of the R-FSPM motor will be briefly described in Section 2. In Section 3, two remedial operations, namely remedial brushless AC (BLAC) operation and remedial injecting harmonic current (IHC) operation, will be proposed. A co-simulation technique will be adopted in Section 4 to assess the performance of the proposed

R-FSPM motor drive at proposed remedial operations. Then, in Section 5, experimental results will be used to verify the proposed remedial operations of the motor drive. Finally, a conclusion will be drawn in Section 6.

2. R-FSPM MOTOR

Figure 1 shows the structure of the 12/10-pole R-FSPM motor, which has 12 salient poles in the stator, 10 salient poles in the rotor, six-coil windings in the stator and 12 PMs in the stator. The coils wound on the diametrically opposite stator poles are connected in series, forming coils-A1 and -A2, and the R-FSPM motor winding configuration is developed by parallel connecting the two coils. Each coil of the R-FSPM motor has its own power converter and controller, which can operate independently. The R-FSPM motor offers the advantages of simple and rugged rotor structure suitable for high speed applications, concentrated stator windings yielding improved space factor and productivity, fault tolerance and increased torque/weight ratio. This motor actually incorporates the merits as follows:

- Similar to the DSPM motor, the R-FSPM motor offers simple rotor structure, easy cooling in PMs and high power density.
- Different from the DSPM motor, the R-FSPM motor has bipolar winding PM flux-linkage, thus achieving higher power density.
- Similar to the existing fault-tolerant motors, the R-FSPM motor possesses the features of redundant winding structure and

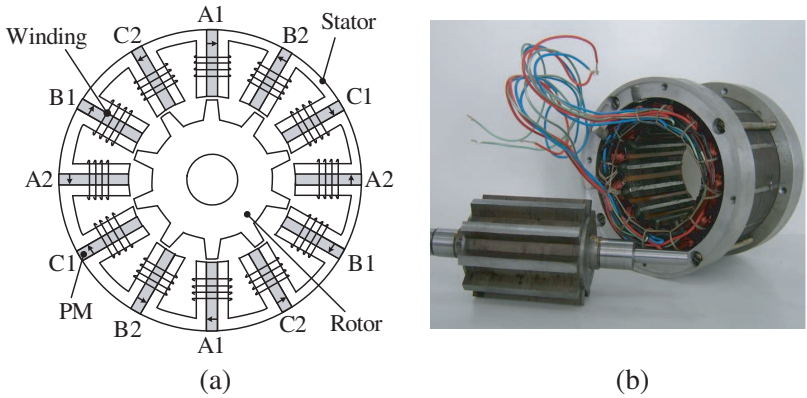

Figure 1. R-FSPM motor. (a) Cross-section. (b) Prototype.

independent phases in electric and magnetic circuits, thus offering the possibility of fault-tolerant operation.

- Different from the most of PM brushless motors having PMs and windings magnetically in series, the R-FSPM motor having PMs and windings magnetically in parallel solves the problem of the influence of armature reaction field on the working point of PMs under the short-circuit fault (shown in Figure 2), hence inherently suitable for high reliability applications.

By using finite element method [17–19], the coil and phase back-EMFs are predicted and shown in Figure 3, comparing with the measured ones. It can be observed that each coil back-EMF has rich harmonic components, but the corresponding phase back-EMF is sinusoidal due to the compensation of harmonic components in the coil back-EMFs. Moreover, back-EMF harmonic analysis is resulted as shown in Figure 4. It can be known that the 2nd harmonic is the main harmonic component, while the 3rd and the higher harmonic can be neglected. Also, the 2nd harmonic amplitude is 15% of the fundamental amplitude and the phase angle is $2\pi/5$. Hence, the back-EMFs of the R-FSPM machine can be expressed as:

$$\begin{cases} e_{a1} = E_1[\sin(\omega_e t) + 0.15\sin(2\omega_e t + 2\pi/5)] \\ e_{b1} = E_1[\sin(\omega_e t + 2\pi/3) + 0.15\sin(2\omega_e t - 4\pi/15)] \\ e_{c1} = E_1[\sin(\omega_e t - 2\pi/3) + 0.15\sin(2\omega_e t - 14\pi/15)] \\ e_{a2} = E_1[\sin(\omega_e t) - 0.15\sin(2\omega_e t + 2\pi/5)] \\ e_{b2} = E_1[\sin(\omega_e t + 2\pi/3) - 0.15\sin(2\omega_e t - 4\pi/15)] \\ e_{c2} = E_1[\sin(\omega_e t - 2\pi/3) - 0.15\sin(2\omega_e t - 14\pi/15)] \end{cases} \quad (1)$$

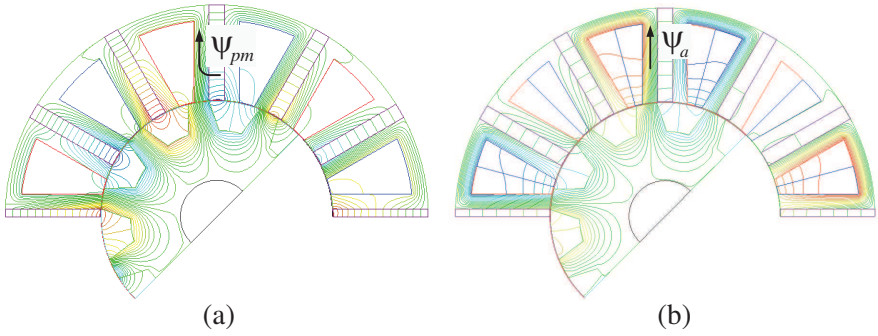

Figure 2. Magnetic field distributions. (a) PMs only. (b) Armature current only.

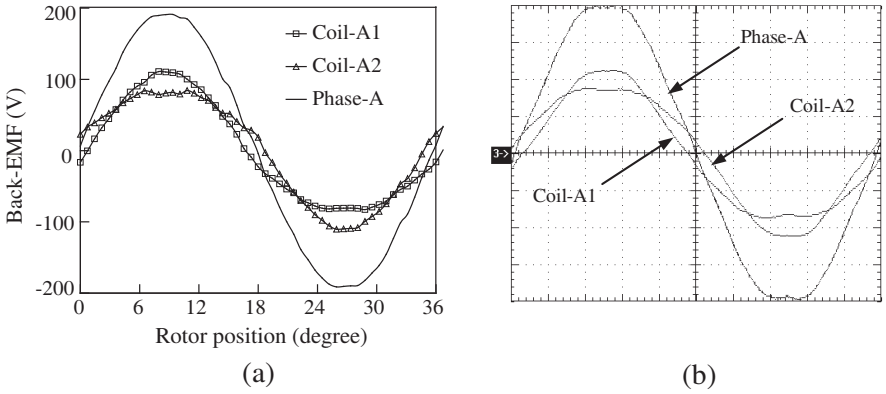

Figure 3. Back-EMF waveforms. (a) Predicted. (b) Measured (0.5 ms/div, 50 V/div).

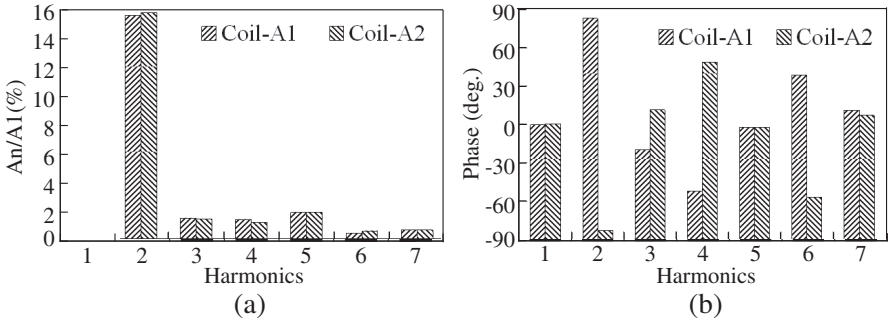

Figure 4. Harmonics analysis. (a) Normalized magnitude. (b) Phase angle.

where E_1 and ω_e are the amplitude and the frequency (the rotor electrical speed) of the fundamental component, respectively.

3. CONTROL STRATEGIES

For the fault-tolerant operation, the proper fault detectors need to be employed. Detailed discussions on the fault detectors for motor drives have been investigated in [20–22]. This work focuses on how to develop the remedial control strategies for the remedial SC operations of R-FSPM motor drives. Firstly, a simple remedial method is proposed by doubling the healthy-coil currents. Secondly, the relationship between the normal BLAC operation before fault and the remedial IHC

operation after fault is derived, and the required harmonic component of the healthy-coil currents are deduced for the torque ripple free operation.

3.1. Normal BLAC Operation

Normally, the R-FSPM motor operates in the dual-channel BLAC operation mode, in which all coils are in work. The six-coil currents can be expressed as:

$$\begin{cases} i_{a1} = I_m \sin(\omega_e t) \\ i_{b1} = I_m \sin(\omega_e t + 2\pi/3) \\ i_{c1} = I_m \sin(\omega_e t - 2\pi/3) \\ i_{a2} = I_m \sin(\omega_e t) \\ i_{b2} = I_m \sin(\omega_e t + 2\pi/3) \\ i_{c2} = I_m \sin(\omega_e t - 2\pi/3) \end{cases} \tag{2}$$

where I_m is the amplitude of the sinusoidal current. For the R-FSPM motors, the motor torque is predominantly resulted from the PM excitation torque since the reluctance torque is negligible. So, the electromagnetic torque under the normal BLAC operation mode can be calculated as:

$$\begin{aligned} T_{en} &= (1/\omega_m) \sum_{p=a}^{c} (e_{p1} \cdot i_{p1} + e_{p2} \cdot i_{p2}) \\ &= [3E_1 I_m - 0.45E_1 I_m \cos(3\omega t + 2\pi/5)]/2\omega_m \\ &\quad + [3E_1 I_m + 0.45E_1 I_m \cos(3\omega t + 2\pi/5)]/2\omega_m = 3E_1 I_m/\omega_m \end{aligned} \tag{3}$$

where ω_m is the rotor mechanical speed. It can be known from (3) that a constant electromagnetic torque is achieved during the normal BLAC operation mode because the harmonic torque of coils counteracts each other.

3.2. Remedial BLAC Operation

Similar to the dual-channel switched reluctance motor [23], the R-FSPM motor can operate in the SC operation mode when its two or three coils in the same channel, such as coils-A1 and -B2, are in fault and disability. In the following analysis, a failure in coils-A2, -B2 and -C2 is considered as an example.

By doubling the healthy-coil currents, the R-FSPM motor can operate in the remedial BLAC operation mode. The currents in the

remedial BLAC operation are:

$$\begin{cases} i'_{a1} = 2I_m \sin(\omega_e t) \\ i'_{b1} = 2I_m \sin(\omega_e t + 2\pi/3) \\ i'_{c1} = 2I_m \sin(\omega_e t - 2\pi/3) \\ i'_{a2} = 0 \\ i'_{b2} = 0 \\ i'_{c2} = 0 \end{cases} \tag{4}$$

Therefore, the remedial BLAC electromagnetic torque can be calculated as:

$$\begin{aligned} T_{er1} &= (1/\omega_m) \sum_{p=a}^{c} \left(e_{p1} \cdot i'_{p1} + 0 \right) \\ &= 3E_1 I_m/\omega_m + 0.45 E_1 I_m \cos(3\omega_e t + 2\pi/5)/\omega_m \end{aligned} \tag{5}$$

It can be concluded from the comparison between (3) and (5) that the proposed remedial BLAC operation can maintain the average torque. However, further observation from (5) reveals that there is a pulsating component in the produced electromagnetic torque, which is a function of the rotor position.

3.3. Remedial IHC Operation

For the torque pulsation free operation, the remedial IHC control strategy is proposed. The key is to operate the R-FSPM motor in the SC operation mode by injecting proper harmonic current to compensate for harmonic torque component in (5).

In the remedial IHC operation mode, the currents are assumed to be:

$$\begin{cases} i''_{a1} = I_1 \sin(\omega_e t) + I_2 \sin(2\omega_e t + \alpha) \\ i''_{b1} = I_1 \sin(\omega_e t + 2\pi/3) + I_2 \sin(2\omega_e t - 2\pi/3 + \alpha) \\ i''_{c1} = I_1 \sin(\omega_e t - 2\pi/3) + I_2 \sin(2\omega_e t + 2\pi/3 + \alpha) \\ i''_{a2} = 0 \\ i''_{b2} = 0 \\ i''_{c2} = 0 \end{cases} \tag{6}$$

where I_1 is the amplitude of fundamental current, and I_2 and α are the amplitude and the harmonic angle relative to the fundamental

component of 2nd harmonic current, respectively. The electromagnetic torque in the remedial IHC operation can be calculated as:

$$T_{er2} = (1/\omega_m)\sum_{p=a}^{c}\left(e_{p1}\cdot i''_{p1}+0\right) = (3/2\omega)\cdot[E_1I_1+E_1I_2\cos(3\omega t+\alpha) +0.15E_1I_1\cos(3\omega t+2\pi/5)+0.15E_1I_2\cos(2\pi/5-\alpha)] \quad (7)$$

To eliminate harmonic torque in (7), a constant electromagnetic torque can be obtained by setting:

$$\begin{cases} \alpha = 2\pi/5 \\ I_2 = -0.15I_1 \end{cases} \quad (8)$$

Thus, by substituting (8) into (7), the remedial IHC torque can be calculated as:

$$T_{er2} = 1.46E_1I_1/\omega_m \quad (9)$$

The torque before and after the fault can be kept the same by setting T_{er2} equal to T_{en}, it yields:

$$I_1 = 2.05I_m \quad (10)$$

Finally, by substituting (8) and (10) into (6), the remedial IHC operation is achieved as:

$$\begin{cases} i''_{a1} = 2.05I_m[\sin(\omega t) - 0.15\sin(2\omega t+2\pi/5)] \\ i''_{b1} = 2.05I_m[\sin(\omega t+2\pi/3) - 0.15\sin(2\omega t-4\pi/15)] \\ i''_{c1} = 2.05I_m[\sin(\omega t-2\pi/3) - 0.15\sin(2\omega t-14\pi/15)] \\ i''_{a2} = 0 \\ i''_{b2} = 0 \\ i''_{c2} = 0 \end{cases} \quad (11)$$

Therefore, it can be concluded that by injecting the 2nd harmonic current, the R-FSPM motor can operate in the remedial IHC operation, in which the restructured fault-tolerant torque can effectively displace the normal torque.

4. SIMULATION

This work adopts the co-simulation modeling method of the magnetic circuit and the electric circuit to asses the performance of the R-FSPM motor drive, in which the system-level simulation is provided [16]. Figure 5 shows the co-simulation model of the R-FSPM motor drive.

To assess the level of the torque ripple under various conditions, a torque ripple factor is defined as follows:

$$K_T = (T_{\max} - T_{\min})/T_{\text{av}} \times 100\% \quad (12)$$

where $T_{\max}$, $T_{\min}$ and T_{av} are the maximum, the minimum and the average values of the output torque, respectively.

Under the normal condition, the R-FSPM motor drive operates in the conventional BLAC operation mode. Based on the developed co-simulation model, the motor current and torque waveforms are simulated as shown in Figure 6. It can be seen the corresponding K_T of the motor drive is 58.3%.

During the loss of one channel, the R-FSPM motor operates in the remedial SC operation mode. The average torque can be maintained by doubling the currents of the healthy-channel. Without taking harmonic

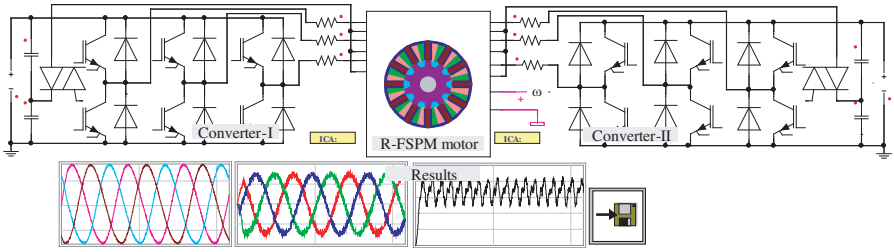

Figure 5. Co-simulation model of R-FSPM motor drive.

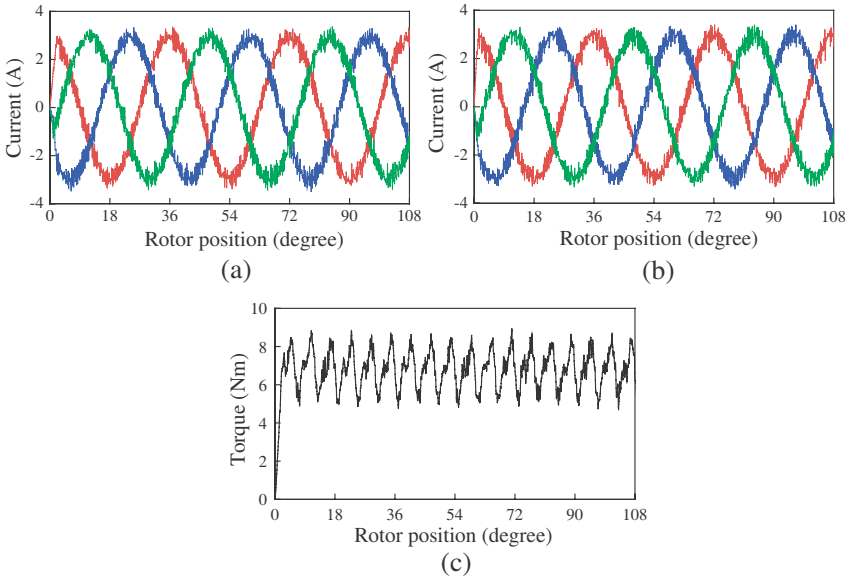

Figure 6. Waveforms at normal operation. (a) Currents of coils-A1, -B1 and -C1. (b) Currents of coils-A2, -B2 and -C2. (c) Torque.

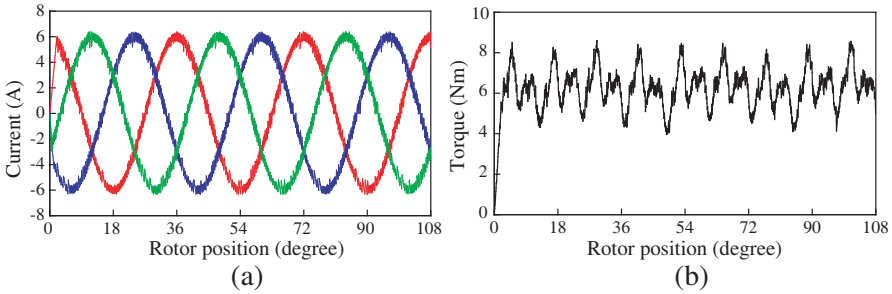

Figure 7. Waveforms at remedial BLAC operation. (a) Currents of coils-A1, -B1 and -C1. (b) Torque.

remedial action, the current and torque waveforms of this R-FSPM motor drive are shown in Figure 7. It can be found that the torque ripple at the remedial BLAC operation is slightly worsening, namely K_T is 70.6%, which is 12.3% larger than the normal torque ripple factor.

By injecting the calculated 2nd harmonic current, the proposed remedial IHC operation is activated. As shown in Figure 8, the corresponding K_T is 62.1%, which is insignificantly larger than the normal torque ripple factor. It can be concluded that during the loss of one channel, both of the proposed remedial strategies can retain the average torque and that the IHC operation can reduce the pulsating torque. Moreover, it should be mentioned that the torque pulsation for both remedial SC operations is higher than that for normal operation, but the redundant drive system continues operating safely under loss of up to three coils. This feature is very important in traction and propulsion applications where high reliability is of major importance.

5. EXPERIMENTAL VERIFICATION

To verify the theoretical analysis, an experimental test bed for the R-FSPM motor drive has been developed. Figure 9 is the photo of experimental setup. It is composed of an R-FSPM motor supplied by two independent IPM-based converters, a separately excited dc generator used as variable load and a transient torque transducer mounted between the R-FSPM motor and the dc generator to measure the torque of the proposed motor drive.

Firstly, the steady-state performances of the R-FSPM motor drive are evaluated. Figure 10 compares the measured torque and current waveforms in the normal and the proposed remedial operations.

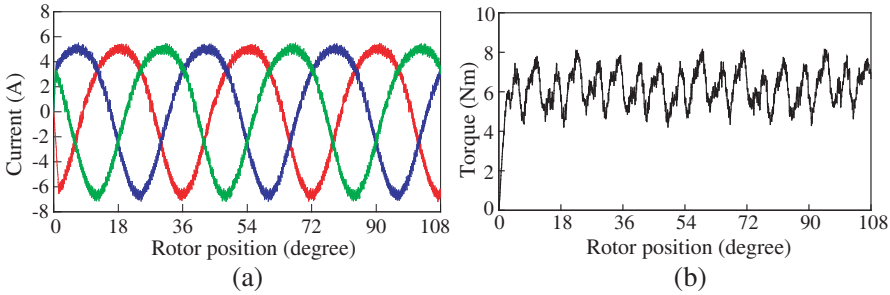

Figure 8. Waveforms at remedial IHC operation. (a) Currents of coils-A1, -B1 and -C1. (b) Torque.

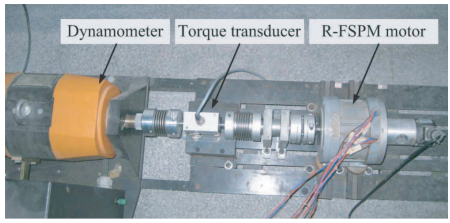

Figure 9. Photo of experimental setup.

As given in (2), the normal current waveforms in Figure 10(a) are sinusoidal in which both of the channels are in work. In the event of one channel loss, the proposed remedial SC operations are activated. For both of the remedial operations, the currents well agree with the theoretical ones. Table 1 compared the theoretical and experimental torque ripple under normal and remedial operations. It should be noted that the measured torque waveforms have a significant discrepancy with those co-simulated ones since the practical and manufacturing conditions are very difficult to be modeled. Nevertheless, it can be known that the proposed remedial operations can maintain the average torque during the loss of one channel, verifying the effectiveness of the proposed fault-tolerant control strategies. Meanwhile, the torque ripple under the remedial BLAC operation is very more than that under the remedial IHC operation due to the effect of harmonic back-EMFs. Also, the remedial IHC operation can reduce torque ripple in the fault-tolerant mode, slightly inferior to the normal operation.

Secondly, the system dynamic performance during the fault occurrence is tested, in which the R-FSPM motor operates from the normal mode to the fault-tolerant modes. Figure 11 reports the healthy-channel current responses, verifying that the R-FSPM motor drive can online switch to the proposed remedial operations.

Finally, it aims to assess whether the R-FSPM motor drive can retain the self-starting capability in the remedial SC operation mode, which is essential for those applications such as EVs desiring frequent start-stop. Figure 12 shows the startup healthy-channel current responses under the remedial BLAC operation and the remedial IHC operation, respectively, showing that the motor drive can successfully perform self-starting during the loss of one channel.

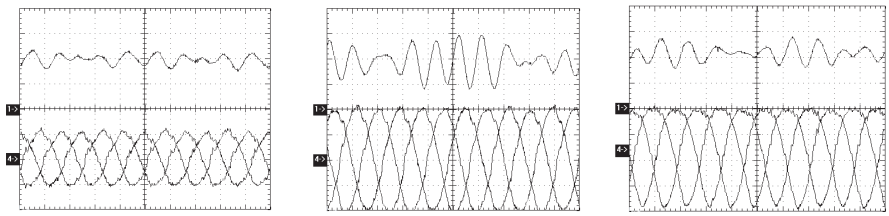

(a) (b) (c)

Figure 10. Measured torque (upper trace) and currents (lower traces) waveforms at various operations (5 ms/div, 3 Nm/div, 3 A/div). (a) Normal BLAC operation. (b) Remedial BLAC operation. (c) Remedial IHC operation.

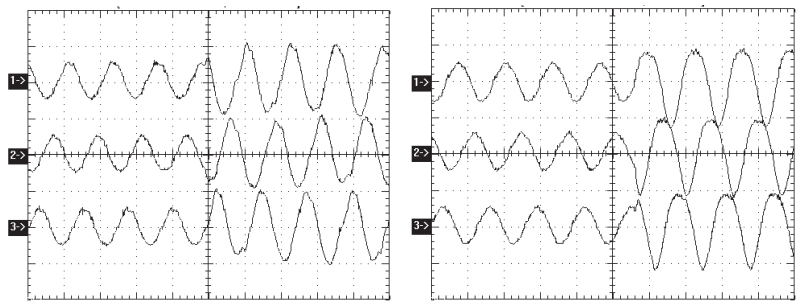

(a) (b)

Figure 11. Measured dynamic current responses from normal operation to remedial operations (5 ms/div, 6 A/div). (a) Remedial BLAC operation. (b) Remedial IHC operation.

Table 1. Comparison of co-simulated and measured torque ripple (%).

	Normal	Remedial BLAC	Remedial IHC
Co-simulated	58.3%	70.6%	62.1%
Measured	43.5%	105.5%	58.8%

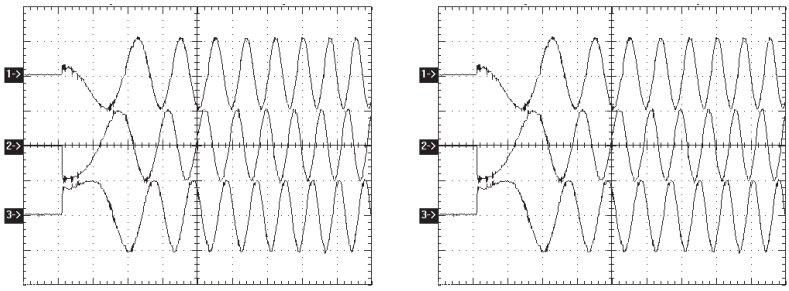

(a) (b)

Figure 12. Measured startup current responses at remedial operations (5 ms/div, 6 A/div). (a) Remedial BLAC operation. (b) Remedial IHC operation.

6. CONCLUSIONS

In this paper, the remedial BLAC and the remedial IHC control strategies have been newly proposed and implemented for fault-tolerant operations of the R-FSPM motor drive. By doubling the health-channel currents, the remedial BLAC operation has been achieved, and its pulsating torque component has been analyzed. By injecting the 2nd harmonic current component into the fundamental current, the remedial IHC operation has also been proposed for torque ripple free operation. The validity of the proposed remedial control strategies has been verified by co-simulation and experimental results. Also, it has revealed that the remedial BLAC operation is simple for implementation, meanwhile the remedial IHC operation offers smooth torque. The proposed remedial operations are particularly important to enable continued operation for many practical applications such as EVs.

ACKNOWLEDGMENT

This work was supported in part by the National Natural Science Foundation of China (Projects 60974060, 50907031 and 51007031), by the Priority Academic Program Development of Jiangsu Higher Education Institutions and by the Professional Research Foundation for Advanced Talents of Jiangsu University, China (Project 10JDG089).

REFERENCES

1. Liu, C., K. T. Chau, and J. Z. Jiang, "A permanent-magnet hybrid brushless integrated starter-generator for hybrid electric vehicles," *IEEE Transactions on Industrial Electronics*, Vol. 57, No. 12, 4055–4064, 2010.
2. El-Refaie, A. M., "Fault-tolerant permanent magnet machines: A review," *IET Electric Power Applications*, Vol. 5, No. 1, 59–74, 2011.
3. Chau, K. T., C. C. Chan, and C. Liu, "Overview of permanent-magnet brushless drives for electric and hybrid electric vehicles," *IEEE Transactions on Industrial Electronics*, Vol. 55, No. 6, 2246–2257, 2008.
4. Touati, S., R. Ibtiouen, O. Touhami, and A. Djerdir, "Experimental investigation and optimization of permanent magnet motor based on coupling boundary element method with permeances network," *Progress In Electromagnetics Research*, Vol. 111, 71–90, 2011.
5. Jian, L., G. Xu, J. Song, H. Xue, D. Zhao, and J. Liang, "Optimum design for improving modulating-effect of coaxial magnetic gear using response surface methodology and genetic algorithm," *Progress In Electromagnetics Research*, Vol. 116, 297–312, 2011.
6. Jack, A. G., B. C. Mecrow, and J. Haylock, "A comparative study of permanent magnet and switched reluctance motors for high-performance fault-tolerant applications," *IEEE Transactions on Industry Applications*, Vol. 32, No. 4, 889–895, 1996.
7. Sun, Z., J. Wang, G. Jewell, and D. Howe, "Enhanced optimal torque control of fault-tolerant permanent magnet machines under flux weakening operations," *IEEE Transactions on Industrial Electronics*, Vol. 57, No. 1, 344–353, 2010.
8. Parsa, L. and H. A. Toliyat, "Fault-tolerant interior-permanent-magnet machines for hybrid electric vehicle applications," *IEEE Transactions on Vehicular Technology*, Vol. 56, No. 4, 1546–1552, 2007.
9. Dwari, S. and L. Parsa, "Fault-tolerant control of five-phase permanent magnet motors with trapezoidal back-EMF," *IEEE Transactions on Industrial Electronics*, Vol. 58, No. 2, 476–485, 2011.
10. Thomas, A. S., Z. Q. Zhu, and G. W. Jewell, "Comparison of flux switching and surface mounted permanent magnet generators for high-speed applications," *IET Electrical Systems*

in Transportation, Vol. 1, No. 3, 111–116, 2011.

11. Cheng M., W. Hua, J. Zhang, and W. Zhao, "Overview of stator-permanent magnet brushless machines," *IEEE Transactions on Industrial Electronics*, Vol. 58, No. 11, 5087–5101, 2011.
12. Zhao, W., K. T. Chau, M. Cheng, J. Ji, and X. Zhu, "Remedial brushless AC operation of fault-tolerant doubly-salient permanent-magnet motor drives," *IEEE Transactions on Industrial Electronics*, Vol. 57, No. 6, 2134–2141, 2010.
13. Zhang, J., M. Cheng, Z. Chen, and W. Hua, "Comparison of stator-mounted permanent-magnet machines based on a general power equation," *IEEE Transactions on Energy Conversion*, Vol. 24, No. 4, 826–834, 2009.
14. Zhu, Z. Q. and J. T. Chen, "Advanced flux-switching permanent magnet brushless machines," *IEEE Transactions on Magnetics*, Vol. 46, No. 6, 1447–1453, 2010.
15. Fei, W., P. C. K. Luk, J. Shen, B. Xia, and Y. Wang, "Permanent-magnet flux-switching integrated starter generator with different rotor configurations for cogging torque and torque ripple mitigations," *Transactions on Industry Applications*, Vol. 47, No. 3, 1247–1256, 2011.
16. Zhao, W., M. Cheng, W. Hua, H. Jia, and R. Cao, "Back-EMF harmonic analysis and fault-tolerant control of flux-switching permanent-magnet machine with redundancy," *IEEE Transactions on Industrial Electronics*, Vol. 58, No. 5, 1926–1936, 2011.
17. Jian, L. and K. T. Chau, "Design and analysis of a magnetic-geared electronic-continuously variable transmission system using finite element method," *Progress In Electromagnetics Research*, Vol. 107, 47–61, 2010.
18. Jian, L., G. Xu, G. Yu, J. Song, J. Liang, and M. Chang, "Electromagnetic design and analysis of a novel magnetic-gear-integrated wind power generator using time-stepping finite element method," *Progress In Electromagnetics Research*, Vol. 113, 351–367, 2011.
19. Mahmoudi, A., N. A. Rahim, and H. W. Ping, "Axial-flux permanent-magnet motor design for electric vehicle direct drive using sizing equation and finite element analysis," *Progress In Electromagnetics Research*, Vol. 122, 467–496, 2012.
20. Vaseghi, B., N. Takorabet, and F. Meibody-Tabar, "Transient finite element analysis of induction machines with stator winding turn fault," *Progress In Electromagnetics Research*, Vol. 95, 1–18, 2009.

21. Torkaman, H. and E. Afjei, "FEM analysis of angular misalignment fault in SRM magnetostatic characteristics," *Progress In Electromagnetics Research*, Vol. 104, 31–48, 2010.
22. Torkaman, H. and E. Afjei, "Hybrid method of obtaining degrees of freedom for radial airgap length in SRM under normal and faulty conditions based on magnetiostatic model," *Progress In Electromagnetics Research*, Vol. 100, 37–54, 2010.
23. Ding, W., D. Liang, and H. Sui, "Dynamic modeling and performance prediction for dual-channel switched reluctance machine considering mutual coupling," *IEEE Transactions on Magnetics*, Vol. 46, No. 9, 3652–3663, 2010.